IOP PUBLISHING NANOTECHNOLOGY
Nanotechnology **18** (2007) 424030 (5pp) doi:10.1088/0957-4484/18/42/424030

Steric effects and chirality in the adsorption of glycine and phenylglycine on Cu(110)

S Blankenburg and W G Schmidt

Theoretische Physik, Universität Paderborn, D-33095 Paderborn, Germany

E-mail: blank@phys.upb.de

Received 5 March 2007, in final form 27 April 2007
Published 21 September 2007
Online at stacks.iop.org/Nano/18/424030

Abstract
Glycine adsorbed on Cu(110) forms (marginally) heterochiral (3 × 2) reconstructed overlayers, in contrast to phenylglycine preferring homochiral adsorption. Density-functional theory within generalized gradient approximation is used to identify the origin of this difference. We find the restriction of the molecular relaxation imposed by the phenyl group in conjunction with intermolecular hydrogen bonds to be responsible.

1. Introduction

Self-organization of organic molecules appears as one of the most promising approaches to the further miniaturization of electronic devices. However, we are only just beginning to understand how the mechanisms of molecular recognition and self-assembly can be exploited for actual device production. In order to investigate molecular self-organization, suitable model systems that allow studying the molecular interactions reproducibly and with high accuracy are needed. Surface adsorbed molecules are an obvious choice. They are accessible to sophisticated surface analysis tools such as scanning tunnelling microscopy (STM) as well as electron diffraction techniques, infrared and other optical spectroscopies. In this context, the physics and chemistry of organic molecules adsorbed on metals is intensively investigated [1–4].

Thereby the simplest amino acid, glycine, is used as prototype for modelling the adsorption of biofunctional molecules on surfaces. For this molecule, the preferred surface adsorption on Cu(110) within a (3 × 2) periodicity is heterochiral [5, 6]. This is in contrast to phenylglycine forming homochiral overlayers on Cu(110) within the same periodicity [7]. This leads to the question why both molecules (shown in figure 1), differing only by the existence of a functional group not involved in the surface bonding, nevertheless prefer different adsorption scenarios. This question is addressed in the present work, using density-functional theory (DFT) within the generalized gradient approximation (GGA).

2. Computational method

We use the Vienna *Ab Initio* Simulation Package (VASP) implementation [8] of DFT-GGA [9]. The electron–ion interaction is described by the projector-augmented wave (PAW) method [10], which allows for an accurate treatment of the first-row elements as well as the Cu 3d electrons with a moderate energy cutoff. We use a value of 400 eV throughout this work. The structure is considered to be in equilibrium when the forces are smaller than 0.03 eV $Å^{-1}$. The Brillouin zone integrations are performed using a 8 × 8 × 8 Monkhorst–Pack mesh for bulk Cu and the Γ point for calculations of the molecules in the gas phase.

For bulk Cu we calculate an equilibrium lattice constant of 3.635 Å and a bulk modulus of 141 GPa in excellent agreement with the experimental values of 3.616 Å [11] and 142 GPa [12], respectively. Given the slight overestimation of the lattice constant and the underestimation of the bulk modulus typical for DFT-GGA, the agreement is excellent.

To model the Cu(110) surface, we use a periodically repeated slab. Each supercell consists of six atomic Cu layers plus the adsorbed molecule and a vacuum region above the surface equivalent in thickness to about 17 atomic Cu layers (≡19.75 Å). Six Cu layers are necessary to describe the relaxation of the Cu surface atoms correctly, i.e., to reproduce the measured trend of the layer spacing oscillations. The calculations are performed using the calculated Cu equilibrium lattice constant. The top five layers of the slab as well as the molecule atoms are allowed to relax. For the Brillouin zone

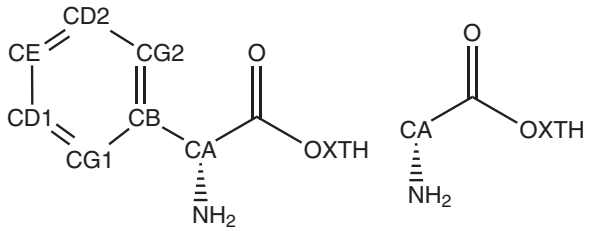

Figure 1. Notation of atoms used here for phenylglycine (left) and glycine (right).

integrations we used a $3\times3\times1$ Monkhorst–Pack mesh. Dipole corrections were applied in all surface calculations to account for the fact that the admolecules are present on one side of the surface slab only.

3. Results and discussion

When racematic mixtures of R- and S-phenylglycine are dosed on the clean Cu(110) surface, two periodicities show up: $\begin{pmatrix}5 & -3\\ 4 & 1\end{pmatrix}$ and $\begin{pmatrix}5 & 3\\ 4 & -1\end{pmatrix}$, suggesting the phase separation of the two enantiomers [13]. Annealing the surface above 420 K causes a phase transition to a (3×2) periodicity. From the experiment it is not clear whether the phase separation of the enantiomers is maintained or not after annealing. Theoretical studies [7], however, show that for the (3×2) periodicity the homochiral surface is energetically slightly preferred.

In contrast, the adsorption of glycine on Cu(110) surface leads to the formation of a heterochiral surface with (3×2) periodicity as shown by x-ray photoelectron diffraction (XPD) measurements [5] and total-energy calculations [6]. Why does an amino acid prefer a different chirality upon adsorption by adding one functional group (phenyl) that is seemingly not involved in the surface bonding?

To answer this question, it is necessary to analyse the different adsorption sites and the intermolecular interactions in detail. We focus in the present study on the adsorption of the deprotonated species. Furthermore, we define one and two admolecules within a (3×2) surface periodicity as half (0.5 ML) and full monolayer (1.0 ML), respectively.

3.1. Phenylglycine

The geometry optimization of a single admolecule on the Cu(110)(3×2) surface leads to the structure shown in the left part of figure 2 in agreement with former results [7]. Thereby, the phenylglycine molecule with a deprotonated carboxyl group about 2.5 Å above the surface was used as starting configuration and a number of different initial positions were probed.

The phenyl-group plane is calculated to be close to the surface normal (tilted by 8.5°) and the carboxyl group is tilted with respect to the surface plane (by 27.6°), in agreement with the interpretation of the data measured for the $\begin{pmatrix}5 & -3\\ 4 & 1\end{pmatrix}$ adsorption structure [14]. The calculated tilt angle between the amino group and the surface amounts to 31.8°, smaller than found experimentally [14].

The adsorption energy calculated from $E_{\mathrm{ad}} = E_{\mathrm{ads/subs}} - E_{\mathrm{subs}} - E_{\mathrm{ads}} + \frac{1}{2}E_{\mathrm{H_2}}$, where E_{ads}, E_{subs}, $\frac{1}{2}E_{\mathrm{H_2}}$, and $E_{\mathrm{ads/subs}}$ refer to the energies of phenylglycine in gas phase, the relaxed copper surface, the hydrogen, and the total system, respectively, is −1.04 eV.

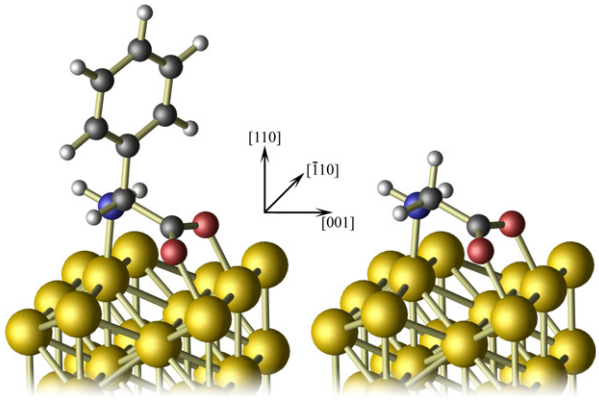

Figure 2. Minimum-energy position of phenylglycine (left) and glycine (right) adsorbed on Cu(110) for the half-monolayer case.

Next we turn to the case of two molecules adsorbed in a (3×2) surface unit cell. Here we used enantiopure and racematic phenylglycine to produce the homochiral (respectively the heterochiral) surface. A large number of molecular starting configurations were probed and the rotational profiles of the phenyl groups were sampled. The most stable hetero- and homochiral structures are shown in figure 3. We calculate adsorption energies of $E_{\mathrm{ad,hetero}} = -1.10$ eV and $E_{\mathrm{ad,homo}} = -1.18$ eV, respectively. Due to the closer packing, adsorption sites different from the half-monolayer case are assumed by the admolecules. In addition, intermolecular hydrogen bonds may form. In figure 3 we indicate potential hydrogen bonds provided that they satisfy the following criteria: (i) $d(\mathrm{D}-\mathrm{A}) < 3.30$ Å and (ii) $\measuredangle(\mathrm{D–H}\cdots\mathrm{A}) > 110°$ (D: donator, A: acceptor). Apart from these geometrical criteria, the formation of hydrogen bonds should lead to some charge polarization with respect to single adsorbed molecules. The respective charge-density differences

$$\Delta\rho(\mathbf{r}) = \rho_{\mathrm{tot}}(\mathbf{r}) - \rho_{\mathrm{ads_1,substr}}(\mathbf{r}) - \rho_{\mathrm{ads_2,substr}}(\mathbf{r}) + \rho_{\mathrm{substr}}(\mathbf{r}), \quad (1)$$

with ρ_{tot}, $\rho_{\mathrm{ads}_i,\mathrm{substr}}$ and ρ_{substr} being the densities of the adsystem with two phenylglycines, of the adsystem with one molecule, and of the clean substrate, respectively, are also shown in figure 3. There is a distinct electron accumulation at some potential hydrogen donors. The Bader theory based on bond critical points (BCP) [15] was additionally applied to identify hydrogen bonds. Based on these criteria, four intermolecular hydrogen bonds form: NH1–O, NH2–O, NH3–O and CH2–O for the homochiral and NH1–O, NH2–O, CH1–O and CH2–O for the heterochiral surface. This conclusion is partially supported by analysing the changes of the molecular CH and NH bond lengths upon adsorption, see table 1. Obviously, the NH bonds stretch upon adsorption, while the CH bonds surface contract. We mention that—in contrast to the case of NH bonds—the CH bond contraction is indicative for the strengthening of the CH···O hydrogen bond [16]. The values of table 1 indicate that the hydrogen bonds of the

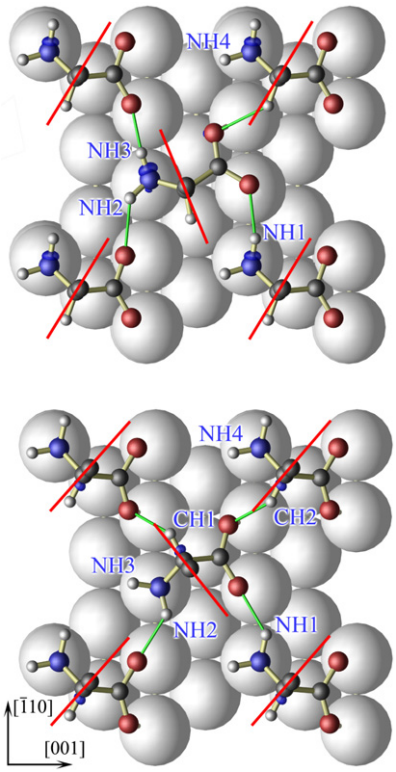

Figure 3. Phenylgycine monolayer adsorbed in a (3 × 2) surface unit cell in homochiral (up) and heterochiral (down) configuration. The phenyl-group orientations and possible hydrogen bonds (see text) are indicated with bars. The total charge-density difference is shown with regions of electron accumulation in blue (isosurface value: $0.04e$ Å^{-3}).

Table 1. NH and CH bond lengths (in Å) of surface-adsorbed and gas-phase phenylglycine molecules, see figure 3 and text.

Bonding	Homochiral ML	Heterochiral ML	In gas phase
NH1	1.033	1.025	1.026
NH2	1.027	1.025	1.026
NH3	1.031	1.025	1.026
NH4	1.025	1.025	1.026
CH1	—	1.091	1.100
CH2	1.096	1.091	1.100

homochiral molecular network are stronger than those of the heterochiral surface.

In order to separate the molecular interaction energy due to hydrogen bonds from the adsorption energy changes resulting from different adsorption positions on the substrate, we calculate $E_{\text{inter}} = E_{\text{tot}} - E_{\text{ads}_1,\text{substr}} - E_{\text{ads}_2,\text{substr}} + E_{\text{substr}}$ with E_{tot}, $E_{\text{ads}_i,\text{substr}}$, and E_{substr} being the energy of the adsystem with two phenylglycine molecules, the energy of the adsystem with one admolecule (1 ML configuration), and the energy of the clean substrate, respectively. It amounts to $E_{\text{inter,homo}} = -0.64$ eV and $E_{\text{inter,hetero}} = -0.36$ eV. Another more quantitatively way to identify hydrogen bonds, see [17–21], is based on Bader's topological paradigm [15]. Here, the strength of the hydrogen bond for closed-shell systems is extracted from the charge density ρ and its Laplacian $\nabla^2\rho$ at the BCP of the selected hydrogen bond. Application of the viral theorem with the kinetic energy density [22]

$$G[\rho] = \tfrac{3}{10}(3\pi^2)^{2/3}\rho^{5/3} + \tfrac{1}{6}\nabla^2\rho \tag{2}$$

results in an expression for the potential energy density

$$V[\rho] = \tfrac{1}{4}\nabla^2\rho - 2G[\rho]. \tag{3}$$

Based on this, an empirical expression for the hydrogen bond dissociation energy, reliable for closed-shell interactions, can be obtained

$$D_E = \tfrac{1}{2}V[\rho]\big|_{\nabla\rho=0}. \tag{4}$$

Using this approach for the calculated BCP's results in an overall dissociation energy of −0.93 eV for the homochiral and −0.85 eV for the heterochiral surface, respectively. We mention, that with the help of this analysis predominately two hydrogen bonds form for each surface: the NH1–O and NH3–O for the homochiral one and the CH1–O and CH2–O for the heterochiral, respectively. The difference between the calculated dissociation energy and the interaction energy obtained from the total energies discussed earlier may be related to various points: (i) the calculated dissociation energy is based on an empirical expression, (ii) the carboxyl groups have a net negative charge due to the deprotonated state leading to a repulsive electrostatic interaction and (iii) there might be a repulsive interaction between the phenyl groups. Nevertheless, both approaches show that indeed the homochiral monolayer is stabilized more by hydrogen bonds than the heterochiral monolayer. While the hydrogen-bond interactions are attractive for the formation of both homo- and heterochiral surface phases, we find a repulsive contribution due to changes of the surface bonding site induced by the closer packing of the molecular overlayer. The energy loss amounts to 0.18 and 0.12 eV per molecule for the homo- and heterochiral monolayer. However, the stronger intermolecular hydrogen bonds in the case of the homochiral surface overcompensate this effect.

3.2. Glycine

The geometry optimization of a single glycine admolecule on the Cu(110)(3 × 2) surface leads to the structure shown in the right part of figure 2 in agreement with former results [6]. Thereby, the glycine molecule with a deprotonated carboxyl group about 2.5 Å above the surface was used as starting configuration and a number of different initial positions were probed. We calculate an adsorption energy of $E_{\text{ad}} = -1.04$ eV for the half-monolayer case, precisely as large as for phenylglycine. Not only the adsorption energies, also the adsorption geometries are very similar for glycine and phenylglycine at low coverage.

This changes for monolayer coverage. In order to analyse the difference between the adsorption scenarios for phenylglycine and glycine, we replaced at first the phenyl group from the phenylglycine with a hydrogen. Without relaxation (except for the new hydrogen) the preferred surface chirality is still homochiral, as for phenylglycine. Hence, there is no direct influence of the phenyl groups on the chirality due to, for example, electrostatic interaction. In the next step we fully relaxed the homo- and heterochiral glycine surfaces, leading to a surprising result: both systems relaxed to a marginally heterochiral configuration, shown in

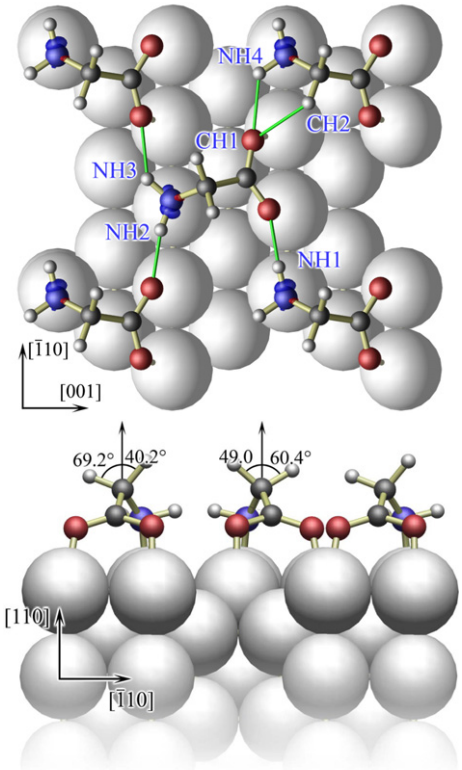

Figure 4. The energetically most favoured structure for one glycine monolayer adsorbed on copper. In the top view (up) possible hydrogen bonds (see text) are indicated with bars. The total charge-density difference is shown with regions of electron accumulation in blue (isosurface value: $0.04e$ Å^{-3}). The side view (down) illustrates the heterochirality of the surface by indicating the angles between the molecular hydrogens and the [110] direction.

Table 2. Atomic N and O positions of surface-adsorbed glycine (in Å) relative to the copper atoms beneath in comparison with the experimental data from [5].

Atom	Direction	Experiment	Present results
N	$\langle\bar{1}\,1\,0\rangle$	0.24 ± 0.10	0.19
			0.19
O	$\langle 0\,0\,1\rangle$	0.68 ± 0.09	0.67
		0.97 ± 0.08	0.92
			0.59
			1.00

figure 4. The calculated geometry is in good agreement with the experimental data from [5], cf table 2.

The intermolecular hydrogen bonds for glycine that satisfy the geometrical criteria mentioned above are indicated in figure 4. Furthermore, the charge-density differences induced by the polarization are shown. A distinct electron accumulation is visible at some potential hydrogen donors. We also calculated the BCP's for this structure. According to these criteria, five intermolecular hydrogen bonds form: NH1–O, NH2–O, NH3–O, NH4–O and CH2–O. This conclusion is supported by analyzing the changes of the molecular CH and NH bond lengths upon adsorption, cf table 3. Obviously, the NH1, NH2, NH3 and NH4 bonds of the homochiral surface stretch upon adsorption, while the CH2–O contract a little bit.

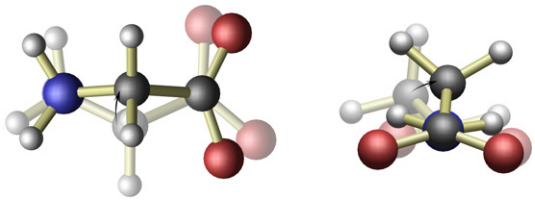

Figure 5. Relaxation and change of tilt angle for glycine upon monolayer adsorption. The transparent molecule represents the initial configuration, the coordinates of which were taken from adsorbed phenylglycine.

Table 3. NH and CH bond lengths (in Å) of surface-adsorbed and gas-phase glycine molecules, see figure 3 and text.

Bonding	Heterochiral ML	In gas phase
NH1	1.031	1.025
NH2	1.030	1.025
NH3	1.027	1.025
NH4	1.025	1.025
CH1	1.096	1.097
CH2	1.096	1.097

We calculate an adsorption energy of $E_{\mathrm{ad}} = -1.23$ eV, larger than for phenylglycine adsorption. The interaction energy of glycine amounts to $E_{\mathrm{inter,hetero}} = -0.81$ eV and the energy loss due to closer packing to 0.20 eV per molecule for the heterochiral surface. The overall dissociation energy calculated from the charge density is -1.01 eV. The analysis of the dissociation energy for each bond shows that predominately three hydrogen bonds form for this surface: the NH1–O, NH2–O and NH3–O. Summarizing, the transition to a full glycine monolayer is energetically more favourable than in the case of phenylglycine and the heterochiral glycine surface has stronger intermolecular interactions, i.e. hydrogen bonds, than both the homo- and heterochiral phenylglycine structures.

3.3. Glycine versus phenylglycine

In order to better understand the differences observed between glycine and phenylglycine adsorption, we use the angle formed by the main molecular plane and the surface (see figure 5) as reaction coordinate and calculate its impact on the surface energetics. As shown in figure 6, two local minima occur for phenylglycine, in contrast to glycine, where only one minimum occurs. In the case of phenylglycine, the two minima are separated by a barrier due to the existence of the phenyl group that prevents the change of chirality observed for glycine. The global minimum for phenylglycine corresponds to the homochiral surface, whereas the global minimum of glycine corresponds to the heterochiral adsorption.

We can now return to the original question why glycine and phenylglycine prefer an opposite chirality upon adsorption. The intermolecular interactions differ substantially between the two heterochiral adsorption configurations. For phenylglycine, predominantly relatively weak CH–O hydrogen bonds are established. In contrast, predominantly strong NH–O hydrogen bonds form between the glycine molecules. These are enabled by the more vertical adsorption position of the latters (cf figure 5). The phenylglycine molecule, on the

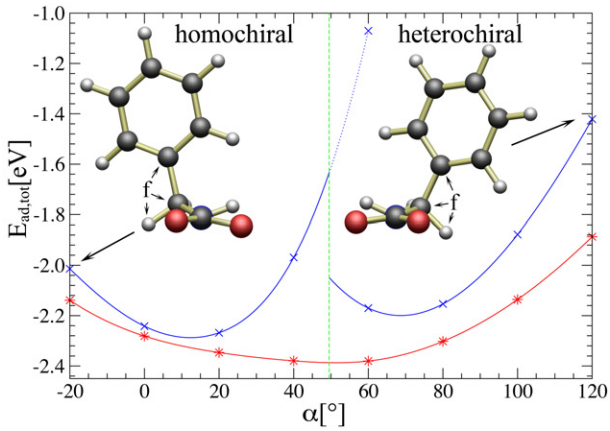

Figure 6. Surface energetics in dependence on the molecular tilt angle (see text) of phenylglycine (crosses) and glycine (asterix). The green line represents the border between the homo- and the heterochiral surface. The solid lines are to guide the eye. Atoms marked with an 'f' are fixed in the [001] direction during relaxation.

other hand, is more tilted due to the existence of the phenyl group and its steric constraints. This renders the formation of homochiral overlayers more favourable. At this point, the comparison with the adsorption of alanine is interesting, where no energetic preference for homo- or heterochiral adsorption was found [23–25]. Therefore, alanine can be viewed as an intermediate between glycine and phenylglycine. Obviously the phenyl group of phenylglycine hinders the molecule more in its rotational freedom than in the case of the methyl group of alanine. The molecular degrees of rotational freedom decrease with the increasing complexity of the additional functional group.

4. Conclusions

Total-energy calculations for homo- and heterochiral surfaces formed by phenylglycine adsorption on Cu(110) show a slight energetic preference of the homochiral surface, in contrast to glycine. In the latter case the heterochiral surface is (marginally) preferred, as shown here in agreement with previous experimental and theoretical investigations [5, 6]. This difference is related to the phenyl group that hinders the relaxation of phenylglycine upon adsorption and thus prevents the formation of strong intermolecular hydrogen bonds.

Acknowledgments

The calculations were done by using grants of computer time from the Paderborn Center for Parallel Computing (PC^2) and the Höchstleistungs-Rechenzentrum Stuttgart. We thank the DFG (SCHM-1361/9) for financial support.

References

[1] Nilsson A and Pettersson L G M 2004 *Surf. Sci. Rep.* **55** 49
[2] Chen Q and Richardson N V 2003 *Nat. Mater.* **2** 324
[3] Schmidt W G, Seino K, Preuss M, Hermann A, Ortmann F and Bechstedt F 2006 *Appl. Phys.* A **85** 387
[4] Preuss M, Schmidt W G and Bechstedt F 2005 *Phys. Rev. Lett.* **94** 236102
[5] Tomes R L, Kang J H, Woodruff D P, Polcik M, Kittel M and Hoeft J T 2003 *Surf. Sci. Lett.* **522** L9
[6] Rankin R B and Sholl D S 2003 *Surf. Sci.* **548** 301
[7] Blankenburg S and Schmidt W G 2006 *Phys. Rev.* B **74** 155419
[8] Kresse G and Furthmüller J 1996 *Comput. Mater. Sci.* **6** 15
[9] Perdew J P, Chevary J A, Vosko S H, Jackson K A, Pederson M R, Singh D J and Fiolhais C 1992 *Phys. Rev.* B **46** 6671
[10] Kresse G and Joubert D 1999 *Phys. Rev.* B **59** 1758
[11] *Landolt Börnstein-Group III Condensed Matter* 1998 vol 14a (Berlin: Springer)
[12] Simmons G and Wang H 1971 *Single Crystal Elastic Constants and Calculated Aggregate Properties: A Handbook* (Cambridge: MIT Press)
[13] Chen Q, Lee C W, Frankel D J and Richardson N V 1999 *PhysChemComm* **2** 41–4
[14] Chen Q, Frankel D J, Lee C W and Richardson N V 2001 *Chem. Phys. Lett.* **349** 167
[15] Bader R F W 1990 *Atoms in Molecules: A Quantum Theory* (Oxford: Oxford University Press)
[16] Gu Y, Kar T and Scheiner S 1999 *J. Am. Chem. Soc.* **121** 9411
[17] Espinosa E, Molins E and Lecomte C 1998 *Chem. Phys. Rev. Lett.* **285** 170
[18] Espinosa E, Alkorta I, Rozas I, Elguero J and Molins E 2001 *Chem. Phys. Lett.* **336** 457
[19] Espinosa E, Molins E and Lecomte C 1999 *Chem. Phys. Rev. Lett.* **300** 745
[20] Jenkins S and Morrison I 2000 *Chem. Phys. Lett.* **97** 317
[21] Jones G, Jenkins S J and King D A 2006 *Surf. Sci.* **600** L224
[22] Abramov Y A 1997 *Acta Crystallogr.* A **53** 264
[23] Rankin R B and Sholl D S 2005 *Surf. Sci. Lett.* **574** L1
[24] Rankin R B and Sholl D S 2005 *J. Phys. Chem.* B **109** 16764
[25] Jones G, Jones L B, Thibault-Starzyk F, Seddon E A, Ravel R, Jenkins S J and Held G 2006 *Surf. Sci.* **600** 1924